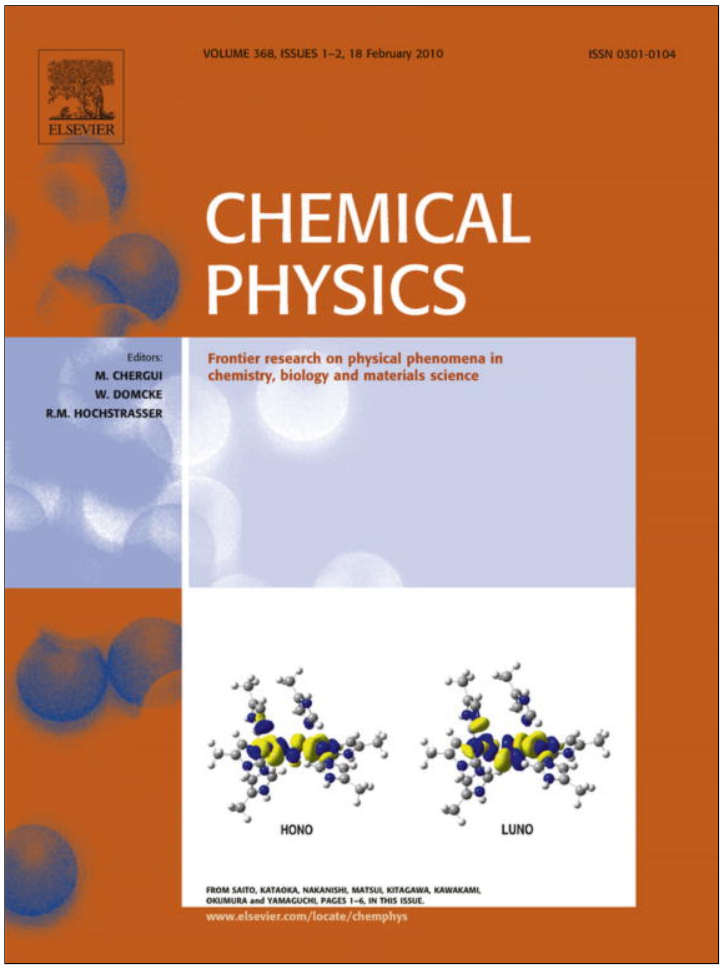

Chemical Physics 368 (2010) 38–48

Contents lists available at ScienceDirect

Chemical Physics

journal homepage: www.elsevier.com/locate/chemphys

Transport coefficients of dilute hydrogen gas, calculations and comparisons with experiments

J. Schaefer

Max-Planck-Institut für Astrophysik, Karl-Schwarzschild-Strasse 1, 85741 Garching, Germany

ARTICLE INFO

Article history:
Received 3 November 2009
In final form 4 December 2009
Available online 16 December 2009

Keywords:
Gases
Transport coefficients

ABSTRACT

The paper presents quantum mechanical ab initio calculations of transport coefficients of dilute H_2 gas, derived from an empirically corrected ab initio interaction potential used in so-called close-coupled channel calculations which provided scattering matrices and subsequently differential scattering cross sections of the elastic and inelastic rotational interactions, for grids of relative kinetic energies sufficient to obtain converged results of transport coefficients at temperatures up to 300 K. The formalism of the Waldmann–Snider theory of the Boltzmann equation has been used following previous work in this field.

Results are presented for the pure *para*- and *ortho*-H_2 gas as well as for their mixtures. Excellent agreement has been found in comparisons with measured results of pure *para*-H_2 gas thus providing proof of the proper input used in the calculations. The comparison with measured normal H_2 transport coefficients was also successful for the calculated normal H_2 shear viscosity (±2%) and the calculated translational heat conductivity coefficient (±2%). Deviations from experiments of up to ≈10% have been found for the total normal H_2 heat conductivity in the temperature range between 75 and 225 K.

1. Introduction

As discussed in the famous elaborate textbook on *Molecular Theory od Gases and Liquids* by Hirschfelder et al. [1], the interchange between the translational and the internal rotational motion in hydrogen gas is weak because of the weak anisotropic interaction of the H_2–H_2 system. It has been shown there that differential cross sections are the crucial input data for determining the transport coefficients which enter the Boltzmann equation of this simplest system of linear molecules, but they were obviously not available when this book has been written. At about the same time when the book appeared, Waldmann and Snider [2a,b,3a] have introduced a generalized Boltzmann equation for particles with degenerate (rotational) degrees of freedom, the Waldmann–Snider equation, to describe Senftleben–Beenakker effects of transport coefficients of polyatomic particles in magnetic fields. A selection of references in [2c–e,3b–e] gives an overview of the further developed theory.

Following the Waldmann–Snider theory, the transport coefficients of the dilute hydrogen gas are determined by collision integrals called relaxation coefficients of the Waldmann–Snider linearized collision operator, and the pertaining cross sections are the "relaxation cross sections". A detailed application of the formalism has already been published by Köhler and Schaefer [4a,b], where the emphasis was on anisotropic transport phenomena of pure parahydrogen gas discussed by using the molecular scattering amplitude matrix. The rotational relaxation cross section, the shear viscosity cross section and the relaxation cross sections of the translational and rotational heat flux contain the double trace of the squared scattering amplitude matrix, i.e., as noted above, only the less voluminous input of differential cross sections is needed for doing quantum mechanical ab initio calculations applied to pure *para*-H_2 and *ortho*-H_2 species and their mixtures. The attempt of doing this is interesting enough for several besides general physical reasons: to show how well we can do with the available tools, especially in calculations of the thermal conductivity coefficients, where several effects contribute, and besides that, there is a request of preparing data for the modelling of astrophysical problems in so-called Molecular Clouds, star-forming regions, together with similar contributions of atomic hydrogen and Helium replacing one of the H_2 molecules.

The interaction potential between the two hydrogen molecules is the crucial starting input for obtaining reasonable quantitative agreement of the calculated results with measured quantities like transport properties discussed here. It has been improved in steps: starting from an ab initio calculated potential energy surface provided by Meyer [5a] and included ab initio results of Liu yielding converged anisotropic spherical expansion terms (in M80), there has been a need of empirical corrections, especially important for the calculations presented in this paper: the isotropic term of the spherical potential expansion has been changed to achieve agreement with low temperature second virial coefficients of *para*-H_2

E-mail address: jas@mpa-garching.mpg.de

0301-0104/$ - see front matter © 2009 Elsevier B.V. All rights reserved.
doi:10.1016/j.chemphys.2009.12.007

gas, by means of a shift of the attractive potential to a slightly smaller distance, followed by a necessary shift of the anisotropic potential terms. The successfully tested resulting "rigid-rotor" potential version has been published [5b] and again empirically fitted with rather small corrections in the attractive potential region to reproduce measured hyperfine transitions of the dimers [5c]. This gave the final potential version used in this paper.

The available measurements for tests of the calculated dilute hydrogen gas transport coefficients are restricted to pure parahydrogen and normal hydrogen gas, whereas the preparation of pure *ortho*-H_2 gas and any gas of fixed *ortho–para* ratio is rather difficult or even impossible. Since the formulae of the transport coefficients are the same for the pure species, we can rely on the converged *ortho*-H_2 results, when agreement with measurements is confirmed for the *para*-H_2 gas. Comparisons of some normal hydrogen gas transport coefficients need extra theoretical expenditure.

Measured rotational relaxation cross sections of parahydrogen gas [7] have been compared with ab initio calculations [4b] before the empirical fit of the isotropic potential was done. The new calculations show now results also of the proper shifts of the anisotropic potential terms obtained after this empirical correction. All the other cross sections of this paper are mainly determined by elastic interactions of the molecules at different rotational states which allows experimentalists to complete a restricted number of measurements within a temperature range and slightly below and above, by using a fitted isotropic interaction potential applied in a simple one-channel integration code, a successful method used e.g. for the interpolations of shear viscosity coefficients.

The paper is ordered as follows: the preparation of the differential cross sections used as input data sets is briefly described in Section 2, Section 3 contains formulae and shows calculated results as well as comparisons with selected measurements of the transport coefficients, each one discussed in a subsection. Results of the comparisons with experiments are discussed in Section 4.

2. Ab initio calculated input data

A 6-term spherical expansion of the interaction potential of the H_2–H_2 system has been used, available after empirical corrections [5b,c] in form of a rigid-rotor approximation:

$$V(\mathbf{R_{ij}},\mathbf{r_i},\mathbf{r_j}) = (4\pi)^{3/2}\sum_{l_1 l_2 K} V_{l_1 l_2 K}(R_{ij},r_i,r_j)\sum_{m_1 m_2 m} C(l_1 l_2 K; m_1 m_2 m) \times Y_{l_1 m_1}(\hat{\mathbf{r}}_\mathbf{i}) Y_{l_2 m_2}(\hat{\mathbf{r}}_\mathbf{j}) Y^*_{Km}(\widehat{\mathbf{R}_\mathbf{ij}}), \quad (1)$$

where $l_1,\ l_2$ range up to 2 and r_i, r_j are confined to the vibrationally averaged distance of the H_2 ground-state (1.449 a.u.). V_{000} is the isotropic potential term, the leading anisotropic terms V_{022} and V_{202} are equal for symmetry reasons, V_{224} is the important quadrupole–quadrupole interaction term and V_{220} and V_{222} are small and less relevant.

The wave function is expanded in a basis of total angular momentum J eigenfunctions with solutions defined by the initial $\alpha' =: j'_1, j'_2, j', l'$ and final (α) quantum numbers

$$\Psi^{JM}_{j'_1 m'_1 j'_2 m'_2}\left(\mathbf{R},\mathbf{r_1},\mathbf{r}_{bf2;\mathbf{k}_{j'_1 j'_2}}\right) = \frac{4\pi}{k_{j'_1 j'_2} R}\sum_{\alpha'\alpha} i^l f^J_{\alpha'\to\alpha}(k_{j_1 j_2} R)\frac{1}{r_1}\chi_{j_1}(r_1)\frac{1}{r_2}\chi_{j_2}(r_2) \times \sum_{m' m_{l'}} I^{JM}_{j_1 j_2 jl}(\hat{\mathbf{r}}_\mathbf{1},\hat{\mathbf{r}}_\mathbf{2},\widehat{\mathbf{R}}) \times C(j'_1 m'_1, j'_2 m'_2/j' m')C(j' m', l' m_{l'}/JM) Y^*_{l' m_{l'}}(\hat{k}_{j'_1 j'_2}), \quad (2)$$

where the Cs are Clebsch–Gordan coefficients, and the Ys are spherical harmonics. The angular part shows the coupling of j_1 and j_2:

$$I^{JM}_{j_1 j_2 jl}(\hat{\mathbf{r}}_\mathbf{1},\hat{\mathbf{r}}_\mathbf{2},\widehat{\mathbf{R}}) = \sum_{m_1 m_2 m m_l} C(j_1 m_1, j_2 m_2/jm)C(jm, lm_l/JM) \times Y_{j_1 m_1}(\hat{\mathbf{r}}_\mathbf{1}) Y_{j_2 m_2}(\hat{\mathbf{r}}_\mathbf{2}) Y_{lm_l}(\widehat{\mathbf{R}}).$$

The angular momenta are coupled in the order of $j_1 + j_2 \to j$, and j is coupled with the orbital angular momentum l to the total J. The ms are magnetic quantum numbers.

H_2 as well as H_2–H_2 are Bose systems, i.e., in case of indistinguishable H_2 molecules in pure *ortho*-H_2 or *para*-H_2 gas the angular part of the wave function must be symmetrized. Symmetrization of these pair wave functions is a basic condition of describing hydrogen gas properties of the pure hydrogen species. Exchange of the molecules gives then a new angular wave function

$$I^{JM(s)}_{j_1 j_2 jl} = [2(1+\delta_{j_1 j_2}\delta_{v_1 v_2})]^{-1/2}\left[I^{JM}_{j_1 j_2 jl}(\hat{\mathbf{r}}_\mathbf{1},\hat{\mathbf{r}}_\mathbf{2},\widehat{\mathbf{R}}) \pm (-1)^{j_1+j_2+j+l} I^{JM}_{j_2 j_1 jl}(\hat{\mathbf{r}}_\mathbf{1},\hat{\mathbf{r}}_\mathbf{2},\widehat{\mathbf{R}})\right], \quad (3)$$

where + in front of (-1) means symmetric, − means antisymmetric wave functions. The weights for parahydrogen are one for symmetric and zero for antisymmetric states, for orthohydrogen we have 2/3 for symmetric and 1/3 for antisymmetric states.

The two restricted symmetrized products, one for $j_1 \leqslant j_2$ and the other one for $j_2 \leqslant j_1$ are angular wave functions of parahydrogen or orthohydrogen free (j_1, j_2) pairs, both contributing to cross sections with equal magnitude.

By substituting Eqs. (1)–(3) into the Schrödinger equation

$$\left[\frac{-\hbar^2\nabla^2_R}{2m_{12}} + H_1(\mathbf{r_1}) + H_2(\mathbf{r_2}) + V(\mathbf{r_1},\mathbf{r_2},\mathbf{R}) - E\right]\Psi(\mathbf{r_1},\mathbf{r_2},\mathbf{R}) = 0, \quad (4)$$

and using the solutions of the single molecule Hamiltonians

$$\left[H_i(\mathbf{r_i}) - E_{vj}\right]\frac{1}{r_i}\chi_{vj}(r_i)Y_{jm}(\hat{\mathbf{r}}_\mathbf{i}) = 0, \quad (5)$$

to integrate over the internal molecular motion and the angles, a (schematic) coupled equations system is obtained

$$\left[\frac{d^2}{dR^2} - \frac{l(l+1)}{R^2} + k^2_\alpha\right] f^J_{\alpha'\to\alpha}(R) = 2\mu\hbar^{-2}\sum_{\alpha''} V^J_{\alpha\alpha''}(R) f^J_{\alpha'\to\alpha''}(R), \quad (6)$$

with

$$\hbar^2 k^2_\alpha = 2\mu(E_{relkin} - (E_\alpha - E_{\alpha'})),$$
$$E_\alpha = E_{j_1} + E_{j_2},$$

and with the reduced mass μ of the system and the potential matrix element $V^J_{\alpha\alpha''}$ [see Ref. [5a], formulae (11) and (12)].

After solving Eq. (6) numerically, the scattering matrices $S^J(E,\alpha,\alpha')$ are computed from the asymptotic $f^J_{\alpha'\to\alpha}(R)$ vectors and their derivatives and stored for subsequent calculations.

In our case we need differential cross sections which are calculated via (space fixed) scattering amplitudes, where the initial asymptotic collision vector $(\widehat{\mathbf{R}} = \hat{\mathbf{e}}')$ is put on the fixed z-axis yielding

$$a^{j_1 j_2 j'_1 j'_2}_{m_1 m_2, m'_1 m'_2}(E,\mathbf{e}) = (\pi/kk')^{1/2} i\sum_{J,l,l'}\sum_{j,j',m,m'} i^{l'-l}(2l'+1)^{1/2} \times C(j'm', l'0/Jm')C(j'_1 m'_1, j'_2 m'_2/j'm')C(j_1 m_1, j_2 m_2/jm) \times C(jm, lm'-m/Jm')[\delta_{\alpha,\alpha'} - S^J(E,\alpha,\alpha')]Y_{lm'-m}(\mathbf{e}). \quad (7)$$

Summation over the ms of the squared amplitudes gives the differential cross section

$$\frac{d\sigma_{j_1 j_2 \leftarrow j'_1 j'_2}}{d\vartheta} = \frac{k}{k'}\frac{a_0^2}{(2j'_1+1)(2j'_2+1)}\sum_{all\ mm'}\left|a^{j_1 j_2 j'_1 j'_2}_{m_1 m_2, m'_1 m'_2}\right|^2 [cm^2] \quad (8)$$

Differential cross sections are stored with a mesh of $\pi/360$ for energy grids reaching up to roughly 2000 wavenumbers (≈7000 m/s relative velocity). Since the full temperature range has been covered from 5 up to 300 K, partial wave expansions for a sufficient number of energy points (60–80) of each rotational H_2 pair state have been done in the calculations.

The formalism of the transport coefficients uses dimensionless rotational energies $\epsilon_i = E_{rot}(j_i)/k_B T$ of the molecule in the rotational state j_i and the energy transfer between the precollisional quantum numbers j_1', j_2' and the postcollisional quantum numbers j_1, j_2 is

$$\Delta\epsilon = \epsilon(j_1') + \epsilon(j_2') - \epsilon(j_1) - \epsilon(j_2) \tag{9}$$

Relative velocities γ are used in units of $\sqrt{2k_BT/\mu}$, and the relation

$$\Delta\epsilon = \gamma'^2 - \gamma^2$$

is valid because of the conservation of energy.

3. Calculations

3.1. Relaxation times

The rotational relaxation time is connected with the effective Waldmann–Snider relaxation cross section $\sigma(0001)$ by the relation [4b]

$$\tau_{rot} = [n v_{th} \sigma(0001)]^{-1}, \tag{10}$$

where n is the particle number density and $v_{th} = \sqrt{8k_BT/\pi\mu}$ is a thermal velocity.

Different kinds of effective cross sections $\sigma(0001)$ have been evaluated because we have normally partial *ortho*- and *para*-H_2 contributions to a general H_2 gas mixture with known mole fractions x_p and x_o. Since kinetic theory provides effective Waldmann–Snider cross sections for rotational relaxation of infinitely dilute molecules, the general expression of the effective cross section becomes [6]

$$\sigma(0001)(H_2) = x_p^2 \sigma\begin{pmatrix}0001|p\\0001|p\end{pmatrix}_p + x_p x_o \left(\sigma\begin{pmatrix}0001|p\\0001|p\end{pmatrix}_{po} + \sigma\begin{pmatrix}0001|o\\0001|o\end{pmatrix}_{op}\right) + x_o^2 \sigma\begin{pmatrix}0001|o\\0001|o\end{pmatrix}_o. \tag{11}$$

By using kinetic theory results [4b], we can write for the pure *ortho*- and *para*-H_2 contributions, marked with k:

$$\sigma\begin{pmatrix}0001|k\\0001|k\end{pmatrix}_k = \frac{2\pi k_B}{c_k^{rot}} Z_k^{-2} \sum_{j_1 j_2 j_1' j_2'} \int\int \exp(-\epsilon_k(j_1) - \epsilon_k(j_2) - \gamma^2)\gamma^2\gamma' \times (\Delta\epsilon)^2 \sum_{all\,m} \left|a^{j_1\, j_2,\, j_1'\, j_2'}_{m_1 m_2, m_1' m_2'}\right|^2 \sin\vartheta\, d\vartheta\, d\gamma \tag{12}$$

In Eq. (12), Z_k is the rotational partition function of the k species, c_k^{rot}/k_B is the rotational heat capacity per molecule $(\overline{\epsilon_k^2} - \overline{\epsilon_k}^2)$. Only rotational inelastic interactions contribute.

Results of the calculated cross sections of pure *para*-H_2 and pure *ortho*-H_2 pairs are shown in Fig. 1, together with reported measurements of Jonkman et al. [7] and Prangsma et al. [8].

The agreement is satisfying in the case of pure *para*-H_2, whereas measurements by Prangsma et al. [8] applied to gas of enriched *ortho*-H_2 give only estimates because the effect of the rest of *para*-H_2 contributing to the sound absorption measurement could not be analyzed properly. This explanation is reasonable, since Eq. (12) is valid for both pure species of hydrogen gas and the result of orthohydrogen is converged as shown in Fig. 1. The two additional terms of Eq. (11) are obtained from the general formalism [6]:

$$\sigma\begin{pmatrix}0001|k\\0001|k\end{pmatrix}_{kl} = \frac{\pi k_B}{c_k^{rot}} \frac{1}{Z_k Z_l} \sum_{j_1 j_2 j_1' j_2'} \int\int \exp(-\epsilon_k(j_1) - \epsilon_l(j_2) - \gamma^2)\gamma^2\gamma' \times (\epsilon_k(j_1') - \epsilon_k(j_1))^2 \sum_{all\,m} \left|a^{j_1\, j_2,\, j_1'\, j_2'}_{m_1 m_2, m_1' m_2'}\right|^2 \sin\vartheta\, d\vartheta\, d\gamma, \tag{13}$$

where the rotational states of the k species can relax and the states of the l species are kept fixed. Rotational double transitions in the mixed pairs have been neglected because their contributions are rather small up to 300 K. Results are shown in Fig. 1.

Half of the forefactor of Eq. (12) in Eq. (13) is generally explained by the fact that the two possible symmetrized wave functions-one for $j_1 \leqslant j_2$ and the other one for $j_2 \leqslant j_1$-contribute in Eq. (12) with equal magnitude.

The *para–para*, the mixed, the *ortho–ortho* and the normal H_2 relaxation cross sections are plotted in Table 1. Since the *ortho–ortho* H_2 cross sections dominate the relaxation of normal hydrogen, they are similar in magnitude to the normal H_2 cross sections.

The rotational cross section $\sigma(0001)$ is also connected with the bulk (or volume) viscosity by the relation [4b]

$$\eta_V = \frac{c_k^{rot}/k_B}{(c_k^{rot}/k_B + 3/2)^2} k_B T \frac{1}{v_{th}\sigma(0001)}, \tag{14}$$

where k_BT stands for p/n. It appears in the Navier–Stokes equation for compressible fluids applied to shock waves. And a Waldmann–Snider cross section determining the translational–rotational coupling of the heat conductivity (see below) can also be expressed with $\sigma(0001)$ [4b].

$$\sigma\begin{pmatrix}1010\\1001\end{pmatrix} = \frac{1}{3}\sqrt{\frac{5c_k^{rot}}{2k_B}}\sigma(0001). \tag{15}$$

3.2. Coefficients of shear viscosity

The shear viscosity coefficient η is essentially determined by the elastic differential cross sections of the H_2 encounters. I may note again that cross section calculations discussed in the rest of this paper are mainly determined by the isotropic potential term fitted to reproduce the second virial coefficients of *para*-H_2 [5b]. The Waldmann–Snider theory provides again an inverse cross section determining the shear viscosity [4a]

$$\eta = \frac{k_b T}{v_{th}} \sigma(2000)^{-1}. \tag{16}$$

The resulting cross section for any mixture of *para–ortho*-H_2 gas is again

$$\sigma(2000)(H_2) = x_p^2 \sigma\begin{pmatrix}2000|p\\2000|p\end{pmatrix}_p + x_p x_o \left(\sigma\begin{pmatrix}2000|p\\2000|p\end{pmatrix}_{po} + \sigma\begin{pmatrix}2000|o\\2000|o\end{pmatrix}_{op}\right) + x_o^2 \sigma\begin{pmatrix}2000|o\\2000|o\end{pmatrix}_o. \tag{17}$$

We use for the pure *para*- and *ortho*-H_2 gas (marked with k) the "viscosity cross section" [4a]:

$$\sigma\begin{pmatrix}2000|k\\2000|k\end{pmatrix}_k = \frac{4\pi}{15}\frac{1}{Z_k^2} \sum_{j_1 j_2 j_1' j_2'} \int\int \exp(-\epsilon_k(j_1) - \epsilon_k(j_2) - \gamma^2)\gamma^2\gamma' \times (\gamma^4 + \gamma'^4 + \gamma^2\gamma'^2(1 - 3\cos^2\vartheta)) \times \sum_{all\,m} |a^{j_1\, j_2,\, j_1'\, j_2'}_{m_1 m_2, m_1' m_2'}|^2 \sin\vartheta\, d\vartheta\, d\gamma. \tag{18}$$

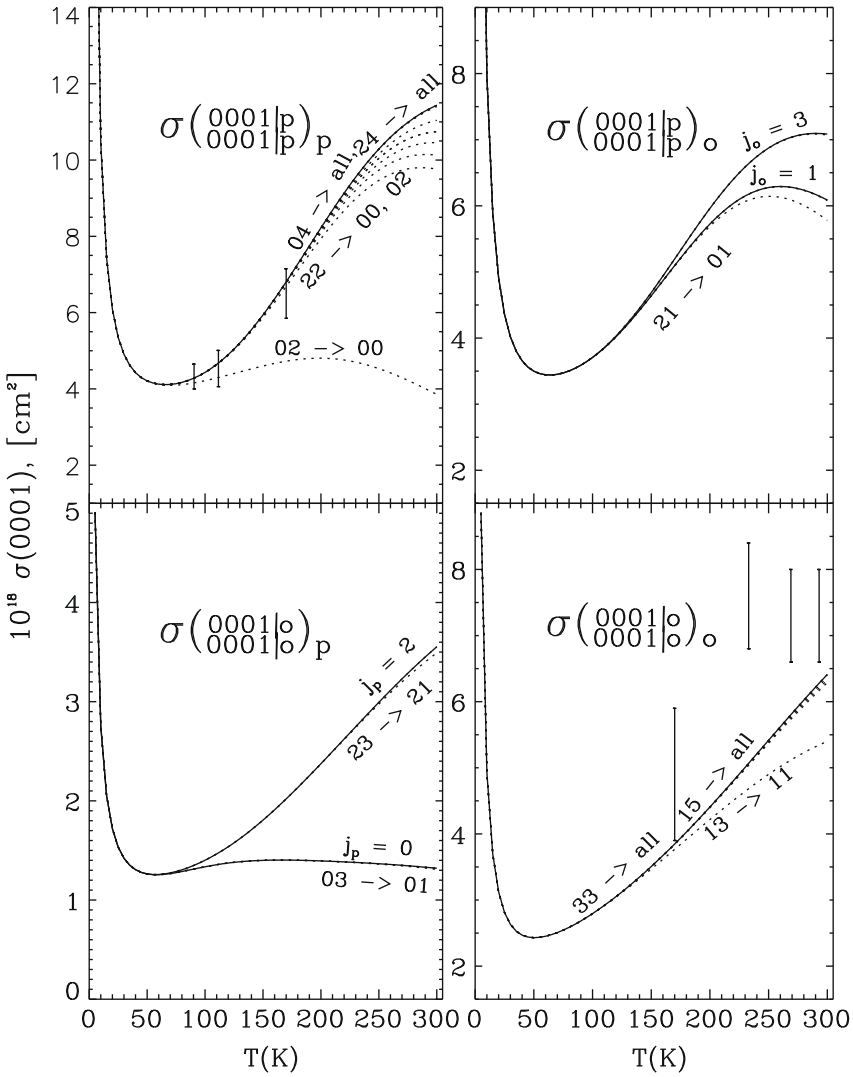

Fig. 1. Calculated relaxation cross sections $\sigma(0001)$ for pure and mixed *para*-H_2 and *ortho*-H_2 gas. The bars show comparisons with measurements [7,8].

A published formula for the mixed terms (Eq. (2.30) in [6]) cannot be applied because the results are obviously useless. Instead we proceed in the same way as in the preceding subsection: The formula for the mixed terms gets an extra factor $1/2$, Z_k^2 is replaced by $Z_k \cdot Z_l$, $\epsilon_k(j_2)$ is replaced by $\epsilon_l(j_2)$, and the l states are kept fixed, the k states can relax, yielding

$$\sigma\begin{pmatrix}2000|k\\2000|k\end{pmatrix}_{kl} = \frac{2\pi}{15}\frac{1}{Z_k Z_l}\sum_{j_1 j_2 j_1' j_2'}\int\int \exp(-\epsilon_k(j_1) - \epsilon_l(j_2) - \gamma^2)\gamma^2\gamma' \times (\gamma^4 + \gamma'^4 + \gamma^2\gamma'^2(1 - 3cos^2\vartheta)) \times \sum_{all\, m} |a^{j_1\ j_2,\ j_1'\ j_2'}_{m_1 m_2, m_1' m_2'}|^2 \sin\vartheta\, d\vartheta\, d\gamma. \quad (19)$$

Calculated results of v_{th} and of the pure and the mixed terms are plotted in Table 2. I may note that differences between results of the pure species are rather small and both are in agreement with measurements [9,10] (see Fig. 2), although one would expect different cross sections because of the different contributions. The difference between the parahydrogen and the normal hydrogen shear viscosities should be within the error bars of the measurements which is ≈2% (Hanley et al. [10]). Consequently, the sum of the mixed terms should be very close to twice the results found for the two pure species. The possibility of $\eta_p > \eta_n$ is discussed below by showing a comparison with a measurement of Kestin and Leidenfrost [11] for normal hydrogen at 293.2 K and with measurements of Becker and Stehl [12].

3.3. Coefficients of heat conductivity

The heat flux contains contributions from the translational and the internal rotational motion of energy and a collisional coupling between them [4b] written

$$\lambda = \lambda_{tr} + \lambda_{rot} + \lambda_{tr,rot}, \quad (20)$$

Again, the coefficients of the heat conductivity are essentially determined by elastic differential cross sections and again, these coefficients are proportional to inverse Waldmann–Snider cross sections. There are essentially two terms to be calculated, the translational and the internal rotational coefficient, whereas the collisional coupling between them will be shown negligible.

The translational heat conductivity is proportional to the inverse effective Waldmann–Snider cross section $\sigma(1010)$ [4a]:

$$\lambda_{tr} = \frac{5}{4}\frac{k_B^2 T}{\mu v_{th}}\sigma(1010)^{-1}, \quad (21)$$

and there are again four terms determining the cross section of the mixed gas:

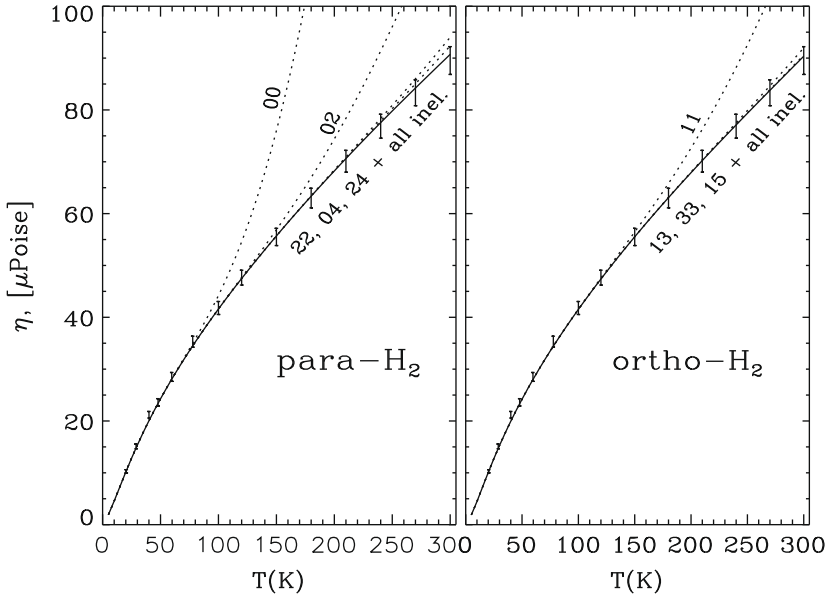

Fig. 2. Calculated shear viscosities of the pure *para*-H_2 and *ortho*-H_2 gas agree both with measurements of Coremans et al. [9] and Hanley et al. [10] as shown with 10% error bars applied to the $\sigma(2000)$ cross section.

$$\sigma(1010)(H_2) = x_p^2\sigma\begin{pmatrix}1010|p\\1010|p\end{pmatrix}_p + x_p x_o\left(\sigma\begin{pmatrix}1010|p\\1010|p\end{pmatrix}_{po} + \sigma\begin{pmatrix}1010|o\\1010|o\end{pmatrix}_{op}\right) + x_o^2\sigma\begin{pmatrix}1010|o\\1010|o\end{pmatrix}_o. \quad (22)$$

The pure *para*- and *ortho*-H_2 terms are obtained from [4a]:

$$\sigma\begin{pmatrix}1010|k\\1010|k\end{pmatrix}_k = \frac{\pi}{15}Z_k^{-2}\sum_{j_1 j_2 j_1' j_2'}\int\int \exp(-\epsilon_k(j_1) - \epsilon_k(j_2) - \gamma^2)\gamma^2\gamma' \times \sum_{all\ m}|a^{j_1\ j_2,\ j_1'\ j_2'}_{m_1 m_2, m_1' m_2'}|^2[11(\Delta\epsilon)^2 + 8\gamma^2\gamma'^2(1-\cos^2\vartheta)]\sin\vartheta\, d\vartheta\, d\gamma. \quad (23)$$

Experimental results for a comparison have been derived by Ditzhuyzen [13] from viscosity measurements, by using the relation

$$\sigma(1010) = \frac{2}{3}\sigma(2000) + \frac{5}{18}\frac{c^{rot}}{k_B}\sigma(0001) \quad (24)$$

which is valid for small nonsphericity interactions and the pure hydrogen species. Since $\sigma(0001)$ is roughly two to three orders of magnitude smaller than $\sigma(2000)$, the neglect in Eq. (24) means an error of <1%. The comparison of measured and calculated results of Eq. (23) is plotted in Fig. 3.

The published formula for the mixed terms (Eq. (2.24) in [6]) turned out to be useless again and we proceed in the same way as in the preceding two subsections yielding

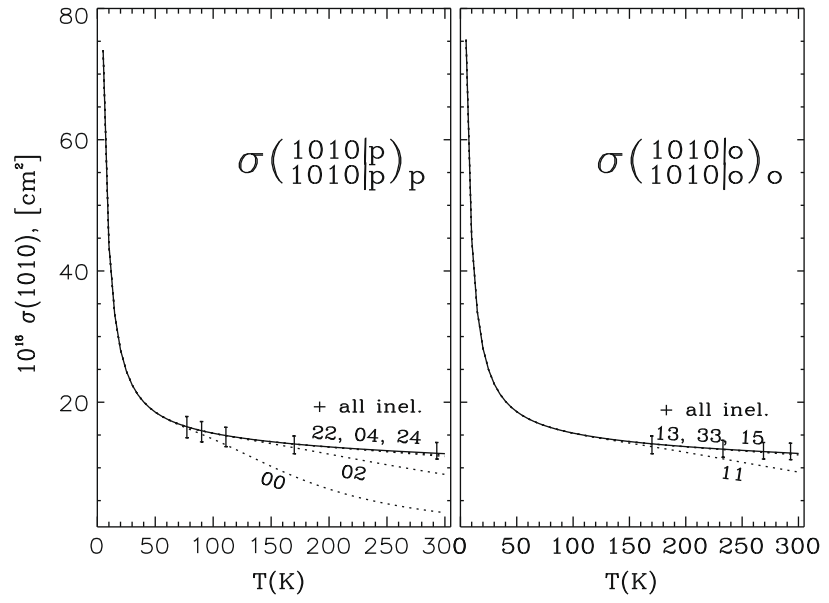

Fig. 3. Calculated cross sections $\sigma(1010)$ of pure *para*-H_2 and *ortho*-H_2 gas. Experimental results with error bars of 10% are used from a collection of Ditzhuyzen [13].

$$\sigma\begin{pmatrix}1010|k\\1010|k\end{pmatrix}_{kl}=\frac{\pi}{30}\frac{1}{Z_kZ_l}\sum_{j_1j_2j_1'j_2'}\int\int\exp(-\epsilon_k(j_1)-\epsilon_l(j_2)-\gamma^2)\gamma^2\gamma'\times\sum_{all\,m}|a^{j_1\,j_2,\,j_1'\,j_2'}_{m_1m_2,m_1'm_2'}|^2[11(\Delta\epsilon_k)^2+8\gamma^2\gamma'^2(1-\cos^2\vartheta)]\sin\vartheta\,d\vartheta\,d\gamma. \quad (25)$$

Eq. (24) is now also valid for the mixed terms as shown in Table 3.

Inelastic differential cross sections contribute very little in the $\Delta\epsilon$ term of Eqs. (23) and (25). We have the same situation as shown in the preceding subsection: the translational heat conductivities of the pure and the mixed gases are practically the same.

The rotational heat conductivity is proportional to the inverse Waldmann–Snider cross section $\sigma(1001)$ [4b]:

$$\lambda_{rot}=\frac{k_B^2T}{2\mu v_{th}}\frac{c_k^{rot}/k_B}{\sigma(1001)}, \quad (26)$$

where $\sigma(1001)$ is again a sum over four terms:

$$\sigma(1001)(H_2)=x_p^2\sigma\begin{pmatrix}1001|p\\1001|p\end{pmatrix}_p+x_px_o\left(\sigma\begin{pmatrix}1001|p\\1001|p\end{pmatrix}_{po}+\sigma\begin{pmatrix}1001|o\\1001|o\end{pmatrix}_{op}\right)+x_o^2\sigma\begin{pmatrix}1001|o\\1001|o\end{pmatrix}_o, \quad (27)$$

and the first and second term must be divided by c_p^{rot}/k_B, the third and fourth term by c_o^{rot}/k_B.

In case of pure *para*-H_2 or *ortho*-H_2 gas we have [4a]:

$$\sigma\begin{pmatrix}1001|k\\1001|k\end{pmatrix}_k=\frac{\pi}{3}\frac{k_B}{c_k^{rot}}Z_k^{-2}\sum_{j_1j_2j_1'j_2'}\int\int\exp(-\epsilon_k(j_1)-\epsilon_k(j_2)-\gamma^2)\gamma^2\gamma'\left[\frac{3}{2}(\Delta\epsilon)^2+\gamma^2(\epsilon_k(j_1)-\epsilon_k(j_2))^2+\gamma'^2(\epsilon_k(j_1')-\epsilon_k(j_2'))^2-2\gamma\gamma'(\epsilon_k(j_1)-\epsilon_k(j_2))(\epsilon_k(j_1')-\epsilon_k(j_2'))\cos\vartheta\right]\times\sum_{all\,m}|a^{j_1\,j_2,\,j_1'\,j_2'}_{m_1m_2,m_1'm_2'}|^2\sin\vartheta\,d\vartheta\,d\gamma. \quad (28)$$

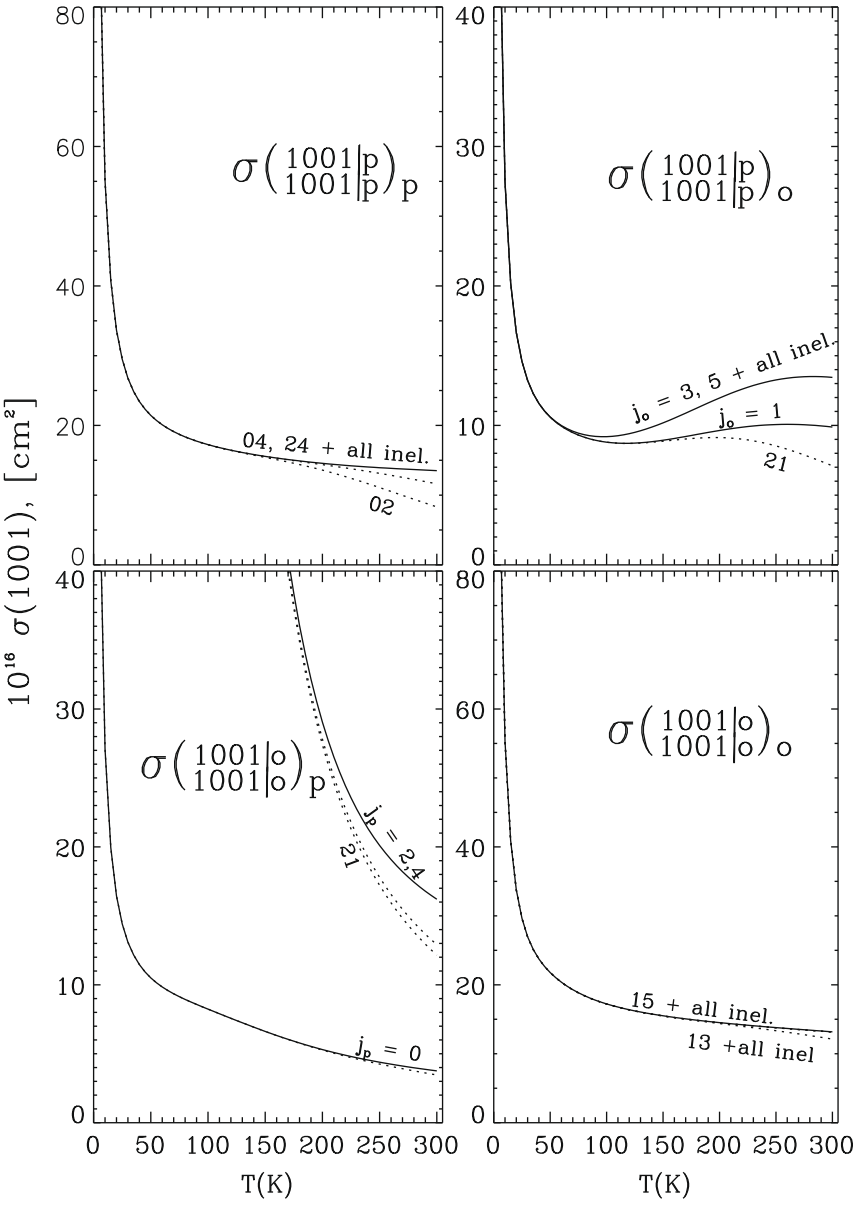

Fig. 4. Calculated cross sections $\sigma(1001)$ of pure and mixed H_2 pairs in the gas.

The cross sections of the two pure species are again almost the same – the difference at 300 K is <3% – and approximately proportional to $\sigma(2000)$ over the whole temperature range (see Fig. 4), although several pairs do not contribute in Eq. (28), as e.g. the pairs $(j_1,j_2)=(0,0)$ and (2,2) for *para*-H_2, and (1,1) and (3,3) for *ortho*-H_2. A successful comparison with experiments (viscosity measurements) has already been published for the case of *para*-H_2 at temperatures up to 200 K [4a].

The cross sections of mixed *para*–*ortho*-H_2 pairs in the gas can be obtained by using one of two possible formulae which give identical results. Formula (a) has been published by Köhler and 't Hooft [6]; we use it with a factor 1/2:

$$\sigma\begin{pmatrix}1001|k\\1001|k\end{pmatrix}_{kl}=\frac{\pi}{6}\frac{k_B}{c_k^{rot}}Z_k^{-1}Z_l^{-1}\sum_{j_1j_2j_1'j_2'}\int\int\exp(-\epsilon_k(j_1)-\epsilon_l(j_2)-\gamma^2)\gamma^2\gamma'\times\left[\frac{3}{2}(\epsilon_k(j_1)-\epsilon_k(j_1'))^2+\gamma^2(\epsilon_k(j_1)-\langle\epsilon_k(j_1)\rangle_0)^2+\gamma'^2(\epsilon_k(j_1')-\langle\epsilon_k(j_1)\rangle_0)^2-2\gamma\gamma'\cos\vartheta(\epsilon_k(j_1)-\langle\epsilon_k(j_1)\rangle_0)(\epsilon_k(j_1')-\langle\epsilon_k(j_1)\rangle_0)\right]\times\sum_{all\,m}|a^{j_1\,j_2,\;j_1'\,j_2'}_{m_1m_2,m_1'm_2'}|^2\sin\vartheta\,d\vartheta\,d\gamma, \tag{29}$$

where the l states are again kept fixed and

$$\langle\epsilon_k\rangle_0=Z_k^{-1}\sum_j(2j+1)\epsilon_k.$$

The four calculated $\sigma(1001)$ cross sections are plotted in Table 4.

The alternative formula (b) of the mixed pairs is again determined the same way as in the preceding three subsections yielding

$$\sigma\begin{pmatrix}1001|k\\1001|k\end{pmatrix}_{l}=\frac{\pi}{6}\frac{k_B}{c_k^{rot}}\frac{1}{Z_kZ_l}\sum_{j_1j_2j_1'j_2'}\int\int\exp(-\epsilon_k(j_1)-\epsilon_l(j_2)-\gamma^2)\gamma^2\gamma'\times\left[\frac{3}{2}(\Delta\epsilon)^2+\gamma^2(\epsilon_k(j_1)-\epsilon_l(j_2))^2+\gamma'^2(\epsilon_k(j_1')-\epsilon_l(j_2'))^2-2\gamma\gamma'(\epsilon_k(j_1)-\epsilon_l(j_2))(\epsilon_k(j_1')-\epsilon_l(j_2'))\cos\vartheta\right]\times\sum_{all\,m}|a^{j_1\,j_2,\;j_1'\,j_2'}_{m_1m_2,m_1'm_2'}|^2\sin\vartheta\,d\vartheta\,d\gamma, \tag{30}$$

The internal rotational heat flux for the normal hydrogen gas contributes the critical part to the comparison of theory and experiment. One reason to be mentioned are the mixed pair cross sections (see Fig. 4) which differ strongly at the lower temperatures, e.g. by a factor of 10^{29} at 5 K, because of the different heat capacities of *para*-H_2 and *ortho*-H_2 (see the second and third column in Table 5) which occur in Eqs. (29) and (30).

The coupling term of the translational and the internal rotational heat conductivity is [4b]

$$\lambda_{tr,rot}=\sqrt{\frac{5}{2}\frac{c_k^{rot}}{k_B}}\frac{k_B^2T}{\mu\nu_{th}}\frac{\sigma\begin{pmatrix}1010\\1001\end{pmatrix}}{\sigma(1010)\sigma(1001)}$$

which can be expressed by making use of Eq. (15) yielding

$$\lambda_{tr,rot}=\frac{5}{6}\frac{k_B^2T}{\mu\nu_{th}}\frac{c_k^{rot}/k_B\sigma(0001)}{\sigma(1010)\sigma(1001)} \tag{31}$$

where again c_p^{rot}/k_B has to be multiplied to the first and second term of the relaxation cross section $\sigma(0001)$ in Eq. (11) and c_o^{rot}/k_B to the third and fourth term. Now we have all cross sections available to calculate the three heat conductivity terms for any *para*–*ortho*-H_2 mixture, for any temperature up to 300 K, and for comparisons with measurements.

Eqs. (23), (28) and (31) can be tested by comparing results of the pure *para*-H_2 gas with measurements of Roder and Diller [14] and of Hanley et al. [10] (see Fig. 5). The agreement is excellent.

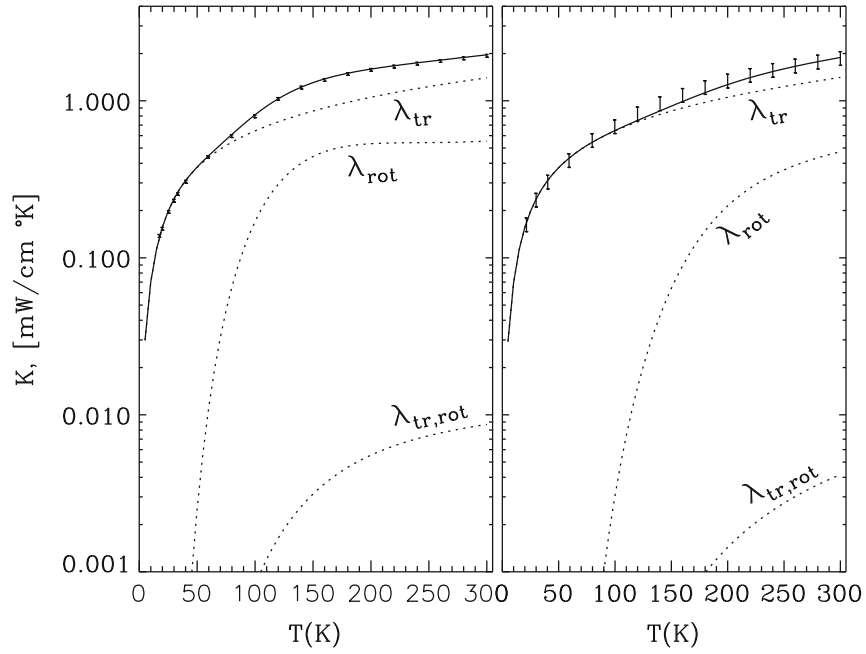

Fig. 5. Calculated heat conductivities summed up from the translational (λ_{tr}), the internal rotational (λ_{rot}) and the collisional coupling term ($\lambda_{tr,rot}$) are plotted vs. temperature. Comparisons with measurements [10,14] are shown for parahydrogen (left, with error bars of ±2%) and for normal hydrogen (right, with error bars of ±10%).

Table 1
Ab initio calculated relaxation cross sections $\sigma(0001)$ times 10^2 (Å^2) of *para–ortho* H_2 gas. The columns have to be multiplied with the known mole fractions according to Eq. (11).

T (K)	*pp*	*po + op*	*oo*	Normal	T (K)	*pp*	*po + op*	*oo*	Normal
5	20.958	19.407	8.857	9.931	155	6.146	6.668	3.589	3.653
10	10.447	10.721	4.929	5.436	160	6.360	6.848	3.673	3.748
15	7.434	7.943	3.696	4.033	165	6.581	7.031	3.760	3.844
20	6.087	6.629	3.124	3.381	170	6.808	7.216	3.847	3.943
25	5.352	5.893	2.813	3.022	175	7.039	7.404	3.937	4.043
30	4.905	5.442	2.633	2.808	180	7.273	7.592	4.028	4.144
35	4.618	5.152	2.528	2.676	185	7.510	7.780	4.121	4.246
40	4.426	4.962	2.469	2.596	190	7.748	7.967	4.215	4.349
45	4.296	4.839	2.440	2.548	195	7.986	8.153	4.310	4.452
50	4.210	4.762	2.431	2.523	200	8.222	8.336	4.407	4.555
55	4.155	4.718	2.436	2.515	205	8.456	8.515	4.504	4.659
60	4.124	4.701	2.452	2.519	210	8.686	8.690	4.603	4.762
65	4.112	4.704	2.477	2.532	215	8.912	8.861	4.703	4.864
70	4.117	4.724	2.507	2.554	220	9.132	9.026	4.803	4.965
75	4.137	4.759	2.544	2.582	225	9.345	9.184	4.904	5.065
80	4.170	4.807	2.586	2.617	230	9.552	9.336	5.006	5.163
85	4.217	4.866	2.633	2.657	235	9.749	9.480	5.109	5.260
90	4.277	4.937	2.683	2.702	240	9.939	9.618	5.211	5.356
95	4.349	5.018	2.737	2.752	245	10.119	9.747	5.314	5.449
100	4.434	5.109	2.795	2.807	250	10.289	9.868	5.416	5.540
105	4.531	5.210	2.855	2.866	255	10.449	9.982	5.519	5.629
110	4.641	5.320	2.918	2.929	260	10.599	10.086	5.621	5.715
115	4.764	5.439	2.984	2.996	265	10.739	10.183	5.723	5.800
120	4.898	5.567	3.052	3.067	270	10.868	10.271	5.824	5.881
125	5.045	5.703	3.122	3.141	275	10.987	10.352	5.924	5.960
130	5.203	5.847	3.195	3.219	280	11.096	10.424	6.024	6.036
135	5.372	5.999	3.270	3.300	285	11.195	10.489	6.122	6.110
140	5.551	6.157	3.347	3.384	290	11.285	10.546	6.220	6.181
145	5.740	6.322	3.426	3.471	295	11.365	10.596	6.316	6.250
150	5.939	6.493	3.506	3.561	300	11.436	10.639	6.411	6.315

Table 2
Ab initio calculated relaxation cross sections $\sigma(2000)$ (Å^2) of *para–ortho*-H_2 gas. The thermal velocity v_{th} (m/s) is plotted in the second column. The columns have to be multiplied with the known mole fractions according to Eq. (17).

T (K)	v_{th}	*pp*	*po + op*	*oo*	T (K)	v_{th}	*pp*	*po + op*	*oo*
5	324.2	110.470	223.880	112.860	155	1805.1	20.799	41.565	20.866
10	458.5	65.971	133.472	67.440	160	1833.9	20.662	41.298	20.732
15	561.5	50.060	100.426	50.710	165	1862.4	20.530	41.040	20.605
20	648.4	41.946	83.980	42.346	170	1890.4	20.404	40.794	20.482
25	724.9	37.128	74.294	37.413	175	1918.0	20.282	40.556	20.365
30	794.1	33.962	67.944	34.179	180	1945.2	20.165	40.327	20.251
35	857.7	31.727	63.464	31.898	185	1972.0	20.053	40.104	20.142
40	917.0	30.061	60.124	30.201	190	1998.5	19.944	39.889	20.037
45	972.6	28.769	57.530	28.885	195	2024.6	19.838	39.679	19.935
50	1025.2	27.734	55.448	27.832	200	2050.4	19.737	39.476	19.837
55	1075.2	26.885	53.734	26.968	205	2075.9	19.638	39.278	19.741
60	1123.1	26.173	52.294	26.245	210	2101.0	19.543	39.084	19.648
65	1168.9	25.566	51.064	25.629	215	2125.9	19.450	38.894	19.558
70	1213.0	25.040	49.998	25.096	220	2150.5	19.360	38.709	19.470
75	1255.6	24.579	49.064	24.629	225	2174.8	19.273	38.527	19.385
80	1296.8	24.170	48.237	24.216	230	2198.8	19.188	38.348	19.301
85	1336.7	23.804	47.498	23.847	235	2222.6	19.105	38.172	19.220
90	1375.5	23.472	46.831	23.513	240	2246.1	19.025	37.997	19.141
95	1413.1	23.171	46.227	23.210	245	2269.4	18.946	37.825	19.063
100	1449.9	22.893	45.673	22.932	250	2292.4	18.870	37.654	18.987
105	1485.7	22.637	45.165	22.677	255	2315.2	18.795	37.485	18.913
110	1520.6	22.400	44.694	22.440	260	2337.8	18.722	37.316	18.840
115	1554.8	22.178	44.257	22.220	265	2360.2	18.650	37.148	18.768
120	1588.2	21.970	43.849	22.014	270	2382.4	18.580	36.981	18.698
125	1621.0	21.775	43.466	21.821	275	2404.3	18.511	36.812	18.628
130	1653.1	21.591	43.106	21.639	280	2426.1	18.444	36.645	18.560
135	1684.6	21.416	42.765	21.468	285	2447.6	18.377	36.475	18.493
140	1715.5	21.251	42.443	21.306	290	2469.0	18.311	36.306	18.427
145	1745.9	21.093	42.136	21.152	295	2490.2	18.247	36.135	18.362
150	1775.7	20.943	41.844	21.005	300	2511.2	18.182	35.964	18.298

Table 3
Ab initio calculated relaxation cross sections $\sigma(1010)$ ($Å^2$) of *para*–*ortho*-H_2 gas. The columns have to be multiplied with the known mole fractions according to Eq. (22).

T (K)	*pp*	*po*	*op*	*oo*	T (K)	*pp*	*po*	*op*	*oo*
5	73.646	74.627	74.627	75.512	155	13.891	13.887	13.844	13.914
10	43.981	44.491	44.491	45.020	160	13.801	13.799	13.754	13.825
15	33.373	33.476	33.476	33.811	165	13.714	13.716	13.668	13.740
20	27.964	27.993	27.993	28.231	170	13.630	10.693	13.584	13.658
25	24.752	24.764	24.764	24.943	175	13.550	13.558	13.504	13.580
30	22.642	22.648	22.648	22.788	180	13.473	13.483	13.426	13.504
35	21.151	21.155	21.155	21.267	185	13.398	13.411	13.350	13.431
40	20.041	20.042	20.042	20.136	190	13.326	13.341	13.277	13.360
45	19.179	19.177	19.177	19.259	195	13.257	13.274	13.206	13.292
50	18.490	18.483	18.483	18.557	200	13.190	13.208	13.136	13.225
55	17.924	17.912	17.911	17.981	205	13.124	13.145	13.068	13.160
60	17.449	17.432	17.431	17.499	210	13.061	13.083	13.001	13.097
65	17.045	17.023	17.021	17.088	215	13.000	13.022	12.936	13.035
70	16.695	16.668	16.666	16.733	220	12.940	12.963	12.871	12.975
75	16.389	16.358	16.354	16.421	225	12.882	12.906	12.808	12.916
80	16.117	16.083	16.078	16.146	230	12.826	12.849	12.745	12.858
85	15.874	15.838	15.831	15.900	235	12.771	12.794	12.683	12.801
90	15.655	15.618	15.609	15.677	240	12.718	12.739	12.622	12.745
95	15.455	15.418	15.406	15.475	245	12.666	12.686	12.561	12.690
100	15.271	15.235	15.222	15.290	250	12.615	12.633	12.500	12.636
105	15.102	15.067	15.052	15.120	255	12.565	12.580	12.439	12.582
110	14.945	14.912	14.894	14.962	260	12.516	12.529	12.379	12.530
115	14.799	14.769	14.748	14.815	265	12.469	12.477	12.319	12.477
120	14.662	14.635	14.611	14.678	270	12.422	12.426	12.258	12.425
125	14.533	14.509	14.483	14.550	275	12.376	12.375	12.198	12.374
130	14.412	14.391	14.362	14.429	280	12.331	12.323	12.137	12.323
135	14.297	14.279	14.248	14.315	285	12.286	12.272	12.076	12.273
140	14.188	14.174	14.139	14.207	290	12.243	12.221	12.014	12.223
145	14.084	14.073	14.036	14.104	295	12.199	12.169	11.952	12.173
150	13.986	13.978	13.938	14.007	300	12.157	12.117	11.889	12.123

Table 4
Ab initio calculated relaxation cross sections $\sigma(1001)$ ($Å^2$) of *para*–*ortho*-H_2 gas. The columns have to be multiplied with the known mole fractions according to Eq. (27).

T (K)	*pp*	*po*	*op*	*oo*	T (K)	*pp*	*po*	*op*	*oo*
5	94.902	47.865	.45E+31	94.976	155	15.437	10.348	51.150	15.388
10	55.094	27.460	.74E+16	55.294	160	15.321	10.520	47.293	15.274
15	40.752	20.218	.78E+11	40.911	165	15.210	10.697	43.925	15.166
20	33.653	16.659	.24E+09	33.784	170	15.104	10.878	40.968	15.062
25	29.489	14.580	.74E+07	29.631	175	15.003	11.061	38.360	14.963
30	26.767	13.226	.72E+06	26.965	180	14.906	11.245	36.050	14.867
35	24.850	12.276	.14E+06	25.118	185	14.813	11.429	33.996	14.776
40	23.424	11.574	.39E+05	23.748	190	14.725	11.611	32.163	14.687
45	22.317	11.034	.15E+05	22.669	195	14.641	11.790	30.522	14.602
50	21.431	10.608	.67E+04	21.780	200	14.560	11.965	29.048	14.519
55	20.701	10.265	3517.20	21.024	205	14.483	12.134	27.721	14.439
60	20.089	9.988	2058.30	20.370	210	14.410	12.297	26.522	14.361
65	19.565	9.764	1307.40	19.798	215	14.340	12.452	25.436	14.285
70	19.110	9.584	885.68	19.294	220	14.274	12.598	24.451	14.211
75	18.710	9.443	631.69	18.848	225	14.210	12.735	23.555	14.139
80	18.355	9.336	469.74	18.451	230	14.150	12.863	22.738	14.069
85	18.036	9.260	361.48	18.095	235	14.092	12.979	21.991	14.000
90	17.748	9.212	286.20	17.777	240	14.037	13.084	21.307	13.933
95	17.485	9.190	232.05	17.489	245	13.985	13.178	20.680	13.867
100	17.244	9.192	191.98	17.228	250	13.935	13.260	20.103	13.802
105	17.021	9.216	161.57	16.990	255	13.887	13.329	19.571	13.738
110	16.815	9.261	137.99	16.773	260	13.841	13.387	19.080	13.675
115	16.623	9.324	119.37	16.573	265	13.796	13.433	18.625	13.613
120	16.443	9.406	104.42	16.388	270	13.753	13.468	18.203	13.552
125	16.274	9.503	92.24	16.216	275	13.711	13.490	17.811	13.491
130	16.115	9.615	82.193	16.056	280	13.670	13.502	17.446	13.431
135	15.965	9.740	73.809	15.906	285	13.630	13.503	17.105	13.371
140	15.823	9.878	66.744	15.765	290	13.590	13.493	16.785	13.311
145	15.688	10.026	60.738	15.632	295	13.550	13.473	16.485	13.251
150	15.559	10.183	55.591	15.507	300	13.510	13.444	16.203	13.192

The second comparison in Fig. 5 is for normal hydrogen. It shows good agreement at the lower and the higher temperatures, but ≈10% lower theoretical results in the temperature range between 75 and 225 K. This will be discussed in the next section.

4. Discussions and conclusions

Transport coefficients of pure and mixed *ortho*- and *para*-H_2 gas have been calculated by using differential cross sections obtained from ab initio calculated scattering matrices in so-called close-coupled calculations. The interaction potential used was a "rigid-rotor" type with the fixed intra-molecular distance of the vibrationally averaged *para*-H_2 ground-state. We could probably expect to find small corrections obtained from the elastic differential cross sections derived from an improved interaction potential, but comparisons of theory and experiments shown in the paper don't indicate missing potential corrections up to 300 K.

The calculated relaxation cross section $\sigma(0001)$ of parahydrogen shows about the same agreement with measurements [7] as in the previous comparison [4b], though considerable improvements of the interaction potential have still been included. Since the results obtained for *ortho*-H_2 gas are derived from the same formula and convergence with regard to contributions has been shown, the same validity of the relaxation cross section can also be claimed for this hydrogen species. Similar accuracy has been provided for the results of the mixed terms of $\sigma(0001)$.

It is worth showing that calculated results of the shear viscosity coefficient determined by the $\sigma(2000)$ cross section are approximately the same for all kinds of *para*–*ortho*-H_2 gas mixtures over the whole temperature range, within the limits of numerical errors and in agreement with measurements applied to parahydrogen gas. This is amazing. One could expect something different because of the different contributions to the converged cross sections (see Fig. 2). The numerical errors of the ab initio calculations are certainly of the order of $\gtrsim$1%, rotational inelastic contributions to the $\sigma(2000)$ cross section have been found of the order of <0.1%.

The possibility of obtaining a difference between *para*-H_2 and normal H_2 shear viscosities may be discussed in comparisons with measurements of Coremans et al. [9], Hanley et al. [10], Kestin and Leidenfrost [11] and Becker and Stehl [12]. Becker and Stehl reported a relative difference of $\approx 10^{-3}$ at 90 K, with $\eta_p > \eta_n$. This is below the numerical errors of the calculations and even below the uncertainty of the other measurements: Coremans et al. reported 35.9 μP, Hanley et al. 35.62 μP at 80 K; the calculations give 35.24 μP for *para*-H_2, 35.31 μP for *ortho*-H_2 and 35.23 μP for normal H_2. Another comparison uses the measured 88.73 μP for the normal gas at 293 K by Kestin and Leidenfrost [11]. Interpolations in Table 2 give 89.21 μP for *para*-H_2, 88.77 μP for *ortho*-H_2 and 89.22 μP for normal H_2 with ≈0.5% deviation from experiment.

About the same agreement with experiments has been found for the translational heat conductivities resulting from Eqs. (23) and (25). Again the results of the pure hydrogen species and the mixtures are essentially the same, although different contributions are summed up as shown in Fig. 3. The rotational heat conductivities of the pure gases are also quite similar and in excellent agreement with experiment as shown previously for the pure *para*-H_2 gas [4a]. These agreements result from the relationships to the shear viscosity.

Measurements of the combined translational and rotational relaxation of the heat flux as obtained by Roder and Diller [14] and again by Hanley et al. [10] could be used for a successful test in the case of pure parahydrogen and a less successful comparison of experiment and theory in the case of normal hydrogen. The latter is the only case of missing agreement of the calculated cross sections with measurements. As to the details shown in Fig. 5:

Table 5
Heat capacities of *para*- and *ortho*-H_2 (2 and 3 column) as used in the calculations and the ab initio calculated heat conductivity coefficients (mW/cm K) of *para*-H_2 (4 column) and normal H_2 gas (5 column).

T (K)	c_p^{rot}/k_B	c_o^{rot}/k_B	λ_{pp}	λ_n	T (K)	c_p^{rot}/k_B	c_o^{rot}/k_B	λ_{pp}	λ_n
5	.267E−39	.285E−68	.0298	.0293	155	1.44827	.29219	1.3432	.9569
10	.931E−18	.345E−32	.0707	.0694	160	1.46066	.32402	1.3783	.9899
15	.996E−11	.259E−20	.1140	.1131	165	1.46669	.35621	1.4111	1.0235
20	.275E−07	.189E−14	.1571	.1562	170	1.46718	.38853	1.4420	1.0579
25	.288E−05	.565E−11	.1985	.1976	175	1.46296	.42074	1.4708	1.0923
30	.600E−04	.109E−08	.2377	.2368	180	1.45481	.45266	1.4978	1.1273
35	.500E−03	.449E−07	.2749	.2740	185	1.44343	.48410	1.5234	1.1624
40	.236E−02	.702E−06	.3104	.3093	190	1.42950	.51490	1.5475	1.1977
45	.770E−02	.579E−05	.3446	.3429	195	1.41360	.54493	1.5703	1.2329
50	.194E−01	.307E−04	.3783	.3751	200	1.39624	.57406	1.5922	1.2680
55	.404E−01	.118E−03	.4123	.4060	205	1.37788	.60221	1.6132	1.3029
60	.734E−01	.356E−03	.4474	.4357	210	1.35891	.62929	1.6334	1.3374
65	.120E+00	.895E−03	.4843	.4644	215	1.33966	.65524	1.6529	1.3717
70	.181E+00	.195E−02	.5237	.4922	220	1.32039	.68004	1.6720	1.4054
75	.255E+00	.380E−02	.5658	.5192	225	1.30133	.70364	1.6907	1.4388
80	.34062	.00675	.6108	.5455	230	1.28267	.72604	1.7089	1.4716
85	.43563	.01113	.6586	.5712	235	1.26455	.74724	1.7271	1.5040
90	.53705	.01725	.7088	.5966	240	1.24708	.76724	1.7450	1.5359
95	.64188	.02536	.7610	.6217	245	1.23033	.78606	1.7628	1.5672
100	.74716	.03569	.8146	.6468	250	1.21437	.80374	1.7806	1.5981
105	.85016	.04837	.8689	.6719	255	1.19923	.82029	1.7984	1.6286
110	.94852	.06349	.9233	.6973	260	1.18493	.83577	1.8162	1.6586
115	1.04030	.08105	.9773	.7232	265	1.17148	.85021	1.8340	1.6882
120	1.12405	.10098	1.0301	.7496	270	1.15886	.86365	1.8520	1.7175
125	1.19876	.12317	1.0815	.7766	275	1.14708	.87614	1.8701	1.7464
130	1.26385	.14744	1.1310	.8045	280	1.13609	.88773	1.8882	1.7750
135	1.31914	.17360	1.1783	.8332	285	1.12588	.89847	1.9067	1.8034
140	1.36475	.20142	1.2232	.8628	290	1.11641	.90840	1.9251	1.8315
145	1.40106	.23063	1.2657	.8934	295	1.10765	.91758	1.9439	1.8595
150	1.42867	.26097	1.3056	.9247	300	1.09956	.92605	1.9628	1.8873

we have practically the same translational parts for the pure para-hydrogen and the normal hydrogen gas, and the contributions from the pure pairs to the rotational term are also practically the same as shown in Fig. 4. The critical quantities are the remaining mixed terms of the rotational heat conductivity. The essential and most sensitive quantities in the two mixed cross sections are the heat capacities of *para*- and *ortho*-H_2. All the other contributions to λ_{rot} have also been used quite successfully in the calculated shear viscosities and in the translational heat conductivity cross sections. I may claim from that validity also for the calculated total heat flux of normal hydrogen in the temperature range between 75 and 225 K, in contrast to the analysis of the measurements.

References

[1] J.O. Hirschfelder, C.F. Curtiss, R.B. Bird, Molecular Theory of Gases and Liquids, John Wiley & Sons, New York, 1964.
[2] (a) L. Waldmann, Z. Naturforsch. 12a (1957) 660. 13a (1958) 609;
(b) L. Waldmann, Z. Naturforsch. 13a (1958) 609;
(c) S. Hess, L. Waldmann, Z. Naturforsch. Teil A 21 (1966) 1529;
(d) H.H. Raum, W.E. Köhler, Z. Naturforsch. Teil A 25 (1970) 1178;
(e) W.E. Köhler, Z. Naturforsch. Teil A 29a (1974) 1705.
[3] (a) R.F. Snider, J. Chem. Phys. 32 (1969) 1051;
(b) F.R. McCourt, R.F. Snider, J. Chem. Phys 46 (1967) 2387;
(c) F.R. McCourt, R.F. Snider, J. Chem. Phys. 47 (1967) 4117;
(d) A.C. Levi, F.R. McCourt, Physica 38 (1968) 415;
(e) G.E.J. Eggermont, H. Vestner, H.F.P. Knaap, Physica 82A (1976) 23.
[4] (a) W.E. Köhler, J. Schaefer, J. Chem. Phys. 78 (1983) 4862;
(b) W.E. Köhler, J. Schaefer, J. Chem. Phys. 78 (1983) 6602.
[5] (a) J. Schaefer, W. Meyer, J. Chem. Phys. 70 (1979) 344;
(b) J. Schaefer, W.E. Köhler, Z. Phys. D 13 (1989) 217;
(c) J. Schaefer, Astron. Astrophys. 284 (1994) 1015.
[6] W.E. Köhler, G.W. 't Hooft, Z. Naturforsch. 34a (1979) 1255.
[7] R.M. Jonkman, G.J. Prangsma, I. Ertas, H.F.P. Knaap, J.J.M. Beenakker, Physica 38 (1968) 441.
[8] G.J. Prangsma, L.J.M. Borsboom, H.F.P. Knaap, C.J.N. Van Den Meijdenberg, J.J.M. Beenakker, Physica 61 (1972) 527.
[9] J.M.J. Coremans, A. Van Itterbeek, J.J.M. Beenakker, H.F.P. Knaap, P. Zandbergen, Physica XXIV (1958) 557.
[10] H.J.M. Hanley, R.D. McCarty, H. Intemann, J. Res. NBS 74A (1970) 331.
[11] J. Kestin, W. Leidenfrost, Physica 25 (1959) 1033.
[12] E.W. Becker, O. Stehl, Z. Phys. 133 (1952) 615.
[13] P.G. van Ditzhuyzen, Thesis, Leiden.
[14] H.M. Roder, D.E. Diller, J. Chem. Phys. 52 (1970) 5928.